Genes & Diseases (2021) 8, 838–848

Available online at www.sciencedirect.com

ScienceDirect

journal homepage: http://ees.elsevier.com/gendis/default.asp

FULL LENGTH ARTICLE

PTPN18 promotes colorectal cancer progression by regulating the c-MYC-CDK4 axis

Chao Li [b,1], Shang-Ze Li [a,b,1], Xi-Cheng Huang [b], Jie Chen [b], Wenbin Liu [c], Xiao-Dong Zhang [b], Xue-Min Song [a,**], Run-Lei Du [b,*]

[a] *Research Centre of Anesthesiology and Critical Care Medicine, Zhongnan Hospital of Wuhan University, Wuhan, Hubei Province, 430071, PR China*
[b] *Hubei Key Laboratory of Cell Homeostasis, College of Life Sciences, Wuhan University, Wuhan, Hubei Province, 430072, PR China*
[c] *College of Health Sciences and Nursing, Wuhan Polytechnic University, Wuhan, Hubei Province, 430023, PR China*

Received 16 July 2020; received in revised form 11 August 2020; accepted 12 August 2020
Available online 25 August 2020

KEYWORDS
CDK4;
Colorectal cancer;
MYC;
Proliferation;
PTPN18

Abstract Protein tyrosine phosphatase non-receptor type 18 (PTPN18) is often highly expressed in colorectal cancer (CRC), but its role in this disease remains unclear. We demonstrated that PTPN18 overexpression promotes growth and tumorigenesis in CRC cells and that PTPN18 deficiency yields the opposite results *in vitro*. Moreover, a xenograft assay showed that PTPN18 deficiency significantly inhibited tumorigenesis *in vivo*. PTPN18 activated the MYC signaling pathway and enhanced CDK4 expression, which is tightly associated with the cell cycle and proliferation in cancer cells. Finally, we found that MYC interacted with PTPN18 and increased the protein level of MYC. In conclusion, our results suggest that PTPN18 promotes CRC development by stabilizing the MYC protein level, which in turn activates the MYC-CDK4 axis. Thus, PTPN18 could be a novel therapeutic target in the future.

* Corresponding author. College of Life Sciences, Wuhan University, Hubei, Wuhan, 430072, China.
** Corresponding author.
E-mail addresses: sxmcl1018@163.com (X.-M. Song), runleidu@whu.edu.cn (R.-L. Du).
Peer review under responsibility of Chongqing Medical University.
[1] These authors contributed equally to this work.

https://doi.org/10.1016/j.gendis.2020.08.001

Introduction

Increasing attention has been paid to the incidence of colorectal cancer (CRC), which is the fourth most deadly cancer in the world after lung, liver and stomach cancer.[1] Western countries have the highest numbers of CRC cases, but there is also rapid increase in CRC incidence in other parts of the world.[2] The causes of colorectal cancer are complicated. The external causes of CRC include environmental factors[3] and personal features or habits, such as age, diet and genetic factors. Specifically, individuals who have high sugar, fat and alcohol intake are at higher risk of CRC, as well as individuals who do not perform adequate levels of physical exercise.[3] In addition, several critical genes in CRC have high mutation rates, such as c-MYC, KRAS, SMAD4 and BRAF.[4] Genomic instability is also a potential factor of CRC.[1,5] All of these factors cause disruptions in numerous important pathways, such as WNT, PI3K, TGF-β and MAPK,[5–7] which are closely related to the growth and proliferation of tumor cells.[8,9]

The MYC-CDK4 axis is a significant part of the WNT signaling pathway,[10,11] and it is one of the pathways most prone to abnormalities in CRC.[2] CDK4, an important downstream mediator of c-MYC signaling, plays a vital role in the G1/S phases of the cell cycle.[12] The inappropriate overexpression of c-MYC in CRC, which is always induced by WNT pathway activation, enhances the expression of CDK4, thus promoting the proliferation of cancer cells.[13] In addition, MYC stability depends on its phosphorylation at Ser62 and dephosphorylation at Thr58, which also stimulate the MYC pathway.[14]

Protein Tyr phosphatases (PTPs) are enzymes that dephosphorylate phosphor-Tyr in target proteins, which counters the function of protein tyrosine kinases (PTKs).[15] The balance between PTPs and PTKs plays a significant role in controlling signaling pathways, and PTP deregulation causes a large number of diseases, including cancers.[16] PTPN18 is a member of the non-receptor protein tyrosine phosphatase (NRPTP) subfamily[17] that is also known as BDP1 and contains a conserved catalytic region and a PEST domain, allowing it to have important functions in regulating signaling pathways.[18,19] PTPN18 is regarded as a tumor suppressor in breast cancer because of its ability to dephosphorylate HER2.[20–22] However, recent studies have shown that PTPN18 knockdown can inhibit the proliferation of tumors and promote apoptosis in endometrial cancer.[23]

Therefore, we speculate that PTPN18 may exert different functions and have other substrates in different cancers. However, no studies have been performed on the role of PTPN18 in CRC at present, and the function of PTPN18 has not yet been fully investigated. After we found that PTPN18 was highly expressed in CRC tissues, we speculated that PTPN18 overexpression is correlated with tumor development, thus highlighting the need to determine the functions of PTPN18 in CRC.

In this work, we discovered PTPN18 expression deregulation in CRC, and we determined how the expression of PTPN18 influences the phenotype of CRC cells. Furthermore, we revealed that PTPN18 plays a vital role in CRC, which can influence CDK4 expression by regulating the MYC pathway in CRC cells.

Materials and methods

Human tissues

Colorectal cancer tissues and paired noncancerous tissues were obtained from Tongji Medical College of Huazhong University of Science and Technology in a previous study.[24] None of the patients received chemotherapy prior to colectomy. Written informed consent forms were obtained from all patients. This study was approved by the Institutional Review Board at the Tongji Medical College of Huazhong University of Science and Technology, and all methods were performed in accordance with the relevant guidelines and regulations.

Tumor xenograft experiment

BALB/c nude mice were maintained under specific pathogen-free (SPF) conditions. Fifteen BALB/c nude mice (male, 5-week-old) were divided into three groups, and each mouse was subcutaneously injected with the following cell types (5×10^6 cells suspended in 200 μl of PBS) in both flanks: HCT116 PTPN18$^{-/-}$ 1#, HCT116 PTPN18$^{-/-}$ 2# and HCT116 WT. After 10 days, the tumor sizes were measured by Vernier calipers every 3 days, and the tumor volumes were calculated according to the following formula: volume $= 1/2 \times (\text{width}^2 \times \text{length})$. The mice were sacrificed after 4 weeks, and the tumor tissues were collected, photographed and weighed. Then, the tumor tissues were kept for other experiments, such as Western blotting and immunohistochemistry. All experimental procedures involving animals were carried out in accordance with the Guide for the Care and Use of Laboratory Animals and approved by the Animal Care and Use Committee of Wuhan University (Project number: 18120I).

Antibodies and reagents

PTPN18 (CST, #8311, 1:1000), MYC (CST, #13987, 1:1000), CDK4 (CST, #2906,1:1000), Flag (MBL, #M185-3L, 1:5000, 1:500 for IF), HA (MBL, #M180-3, 1:5000), HA (CST, #3724, 1:800 for IF), GAPDH (MBL, #M171-3, 1:1000), Ki67 (CST, # 12202S, 1:400 for IHC), and DAPI (Beyotime, #C1002) were used in our experiments.

Cell lines, plasmids and lentiviral infection

The human colorectal cancer cell line HCT116 (from the ATCC) was cultured in McCoy's 5A medium (AppliChem, Darmstadt, Germany) containing 10% fetal bovine serum (FBS; HyClone, Logan, UT, USA) and 100 U of penicillin–streptomycin (Gibco, Carlsbad, CA, USA). HEK293T cells (from the ATCC) and HeLa cells (from the ATCC) were cultured in complete DMEM (HyClone) containing 10% FBS and 100 U of penicillin–streptomycin. All cells were cultured at 37 °C in a 5% CO_2 incubator.

PTPN18 isoform 2 and full-length MYC were cloned into both pHAGE and PC5-HA vectors, and mutations of PTPN18 were constructed based on PTPN18 isoform 2. The sequences of the primers used to clone PTPN18 isoform 2 into

pHAGE were as follows: forward: 5′-CGACGCGTATGAGCCGCAGCCTGGAC-3′; and reverse: 5′-CCCTCGAGCACCCGGGTCCACTCAGC-3′. The sgRNA for PTPN18 was designed using an open source platform (https://zlab.bio/guide-design-resources) as follows: 5′-GGAAGCTCCGCGCCGAGTCC-3′, and this sgRNA was subsequently cloned into lentiCRISPR v2.

293T cells were transfected with pHAGE-PTPN18 and lentiCRISPR v2-PTPN18 with packaging plasmids (psPAX2 and pMD2.G) to generate the two different lentiviruses. At 48—72 h posttransfection, the cell supernatants containing lentiviruses were collected. Then, HCT116 cells were infected with lentiviruses in the presence of 5 μg/ml polybrene to construct different stable-transfected cell lines.

CCK8 assay

Cell proliferative ability was determined using a cell counting kit-8 (CCK-8, Bimake, #B34304). Each group of cells (1×10^3 cells per well) was plated into a 96-well plate in triplicate with the corresponding medium and incubated at 37 °C for seven days. CCK8 reagent was added to the plate (1/10 of the medium) and incubated at 37 °C for 1 h, and the absorbance of the plate was detected at 450 nm.

Colony formation and soft agar assays

To examine the capacity for long-term cell proliferation, each group of cells (400 cells per well) was plated into 6-well plates and incubated at 37 °C for 14 days. Then, a 0.1% crystal violet solution was added to the plates and incubated at 37 °C for 30 min. After washing the plates slowly with water, the visualized colonies could be counted.

A soft agar assay was used to determine the malignant proliferation capacity. Cells were mixed in a 0.3% low-melting agar solution with medium, and the mixture was plated on top of a 0.5% agar base containing medium in six-well plates (3×10^4 cells per well). Then, the cells were incubated at 37 °C for 21 days and photographed with a digital camera coupled to a microscope for counting.

Luciferase reporter assay

293T cells were plated into a 24-well plate at a density of 2×10^5 cells per well and transfected with the indicated plasmids [pRL-TK (10 ng), pGL4-MYC (100 ng), pHAGE/pHAGE-PTPN18 (400 ng)] for 24 h. Then, luciferase lysis buffer was added, and the plate was shaken for 30 min. Luciferase activities were assayed according to the manufacturer's instructions (Promega) using the DLR-O-INJ program in GloMAX, and MYC luciferase activity was normalized to that of TK.

RNA isolation and real-time PCR

Total RNA was extracted from cells and tissues according to the standard TRIzol (TaKaRa, #9109) protocol. Reverse transcription was performed using the Revertaid First Strand cDNA Synthesis Kit (Thermo, #K1622). Quantitative real-time PCR was performed on a Quantagene q225 using MonAmp SYBR Green qPCR MIX (Monad, #RN04006M) according to the manufacturer's instructions. The primers used for real-time PCR were as follows: CDK4: 5′-ATGGCTACCTCTCGATATGAGC-3′ (forward) and 5′-CATTGGGGACTCTCACACTCT-3′ (reverse); and MYC: 5′-GGCTCCTGGCAAAAGGTCA-3′ (forward) and 5′-CTGCGTAGTTGTGCTGATGT-3′ (reverse). β-Actin was used as a control.

RNA sequencing

First, the total RNA samples were treated with DNase I. Then, the mRNA was enriched using oligo(dT) magnetic beads (for eukaryotes). After being mixed with the fragmentation buffer, the mRNA was fragmented into short fragments. Then the first-strand cDNA was synthesized using random hexamer primers, after which buffer, dNTPs, RNase H and DNA polymerase I were then added to synthesize second-strand cDNA. The double-stranded cDNA was then purified with magnetic beads, after which end repair and 3′-end single nucleotide A (adenine) addition was performed. Finally, sequencing adaptors were ligated to the fragments, and the fragments were enriched by PCR amplification. During the QC step, an Agilent 2100 Bioanalyzer and an ABI StepOnePlus Real-Time PCR System were used to qualify and quantify samples of the library, respectively. Subsequently, the library products were sequences using a BGISEQ-500 instrument.

Immunoprecipitation and Western blotting analysis

Cells were lysed with buffer (30 mM Tris-HCl pH 7.4, 150 mM NaCl, and 1% NP40) containing NaF, Na_3VO_4, leupeptin, PMSF, and aprotinin. The cell lysates were incubated on ice for 30 min with mixing every 10 min and then centrifuged at 12,000 g for 15 min at 4 °C. Then, the supernatants were collected and incubated with anti-HA beads (Bimake, #B26202) overnight at 4 °C. The beads were washed 4 times, each time for 5 min, with buffer (30 mM Tris-HCl pH 7.4, 500 mM NaCl, and 1% NP40). Then, the beads were suspended in lysis buffer containing 0.02% blue bromophenol and 2% mercaptoethanol and boiled at 95 °C for 15 min. Subsequently, the supernatants were collected for SDS-PAGE and Western blotting.

Equal amounts of protein were separated by 10% SDS-PAGE and transferred to polyvinylidene difluoride (PVDF) membranes. Then, the PVDF membranes were blocked with 5% milk in TBST and incubated overnight with Flag (MBL, #M185-3L, 1:5000) and HA (MBL, #M180-3, 1:5000) antibodies. After washing with TBST 4 times, the membranes were incubated with an HRP-conjugated secondary antibody in 5% milk in TBST for 1 h at room temperature. Then, the membranes were washed with TBST 3 times (5 min each time), and protein expression was detected using ECL.

Immunofluorescence

HeLa cells were grown on coverslips in a 12-well plate. After washing with PBS, the cells were fixed with cold 4% paraformaldehyde for 5 min at RT. Then, the cells were permeabilized in 0.25% Triton X-100 for 10 min and washed with PBS. The cells were blocked for 30 min at 37 °C with 3%

BSA, followed by incubation with primary antibodies against Flag (MBL, #M185-3L, 1:500) and HA (CST, #3724, 1:800) overnight at 4 °C. On the following day, the coverslips were washed with PBS 3 times (5 min each time) and incubated with anti-rabbit Alexa Fluor 488 (Invitrogen, #A11008) and anti-mouse 594 (Invitrogen, #A11001) at 37 °C for 60 min. Then, the coverslips were stained with DAPI (Beyotime, #C1002) for 30 min at 37 °C. Finally, the coverslips were observed under a fluorescence microscope (Leica).

Immunohistochemistry

First, tissues were fixed in formalin and embedded in paraffin. Then, the tissues were deparaffinized in xylene and rehydrated with an alcohol gradient. Endogenous peroxidase activity was blocked with 3% H_2O_2, and antigens were retrieved with universal antigen retrieval solution for immunohistochemistry. The slices were blocked in 10% goat serum for 30 min at room temperature, incubated with primary antibodies overnight at 4 °C, and incubated with secondary antibody at room temperature for 30 min. Next, the sections were incubated with HRP-conjugated secondary antibodies, and DAB substrate was used for detection with hematoxylin nuclear counterstaining. Sections were visualized by microscopy (OLYMPUS BX53).

Statistical analysis

All statistical analyses were performed using GraphPad Prism v6.0. The differences between groups were analyzed using Student's t-test or one-way ANOVA. $P < 0.05$ was considered statistically significant. Colony numbers were counted using ImageJ. The H-score results from the IHC experiment and Pearson's coefficient of colocalization of IF were analyzed using ImageJ.

Ethics statement

Written patient consent was obtained for publication of this research. The approval for this study was granted by the Ethics Committee of the Tongji Medical College of Huazhong University of Science and Technology.

Data availability

The datasets analyzed during the present study are publicly available in the GEO database (GSE4107) and in GEPIA (http://gepia.cancer-pku.cn/detail.php?gene=PTPN18).

Results

Increased PTPN18 expression in CRC

To examine how PTPN18 expression changes in CRC, we searched the GEO database and observed that the mRNA expression of PTPN18 was increased in early onset colorectal cancer compared to that observed in healthy control tissues (Fig. 1A). Then, real-time PCR was used to verify the mRNA level of PTPN18 in CRC and benign tissues. Specifically, human colorectal cancer tissues and paired normal tissues were collected from 8 patients. After we extracted mRNA from these tissues and real-time PCR was performed, we found that the average mRNA expression of PTPN18 was much higher in cancer tissues than in normal tissues (Fig. 1B). In addition, a Kaplan–Meier analysis demonstrated poorer overall survival for patients with high PTPN18 mRNA expression using Gene Expression Profiling Interactive Analysis (GEPIA) data (Fig. 1C). In sum, the data show that PTPN18 expression was increased and associated with an unfavorable prognosis in CRC.

PTPN18 overexpression leads to increased tumor cell growth

To assess the effect of enhanced PTPN18 expression on CRC cell growth, we constructed HCT116 cell lines overexpressing Flag-PTPN18 and Flag-PTPN18$^{D90A\ C122S}$ by lentiviral transfection. The PTPN18$^{D90A\ C122S}$ mutant is a phosphatase activity deficient mutant in which the aspartate in the "WPD loop" was mutated to alanine (D/A) and the cysteine in the signature motif was mutated to serine (C/S). Furthermore, PTPN18$^{D90A\ C122S}$ is a type of "substrate-trapping" mutant that can be used to detect the substrates of PTPN18.[25] The expression of Flag-PTPN18 and Flag-PTPN18$^{D90A\ C122S}$ was detected by Western blot assay (Fig. 2A). Then, a CCK8 assay was conducted to assess the impact of PTPN18 overexpression on the proliferation of HCT116 cells. The results showed that Flag-PTPN18 overexpression notably promoted the proliferation of HCT116 cells, while Flag-PTPN18$^{D90A\ C122S}$ overexpression slightly inhibited the proliferation of HCT116 cells (Fig. 2B). In addition, we also performed colony formation and soft agar assays. The results showed that more colonies were observed in the Flag-PTPN18-overexpressing groups than that observed in the control groups, while somewhat fewer colonies were observed in the Flag-PTPN18$^{D90A\ C122S}$-overexpressing groups (Fig. 2C and E). The consistent results of both experiments indicated that the growth of HCT116 cells was enhanced by PTPN18 overexpression. Cell numbers were also counted as illustrated in the figures (Fig. 2D and F). These data indicated that the proliferation ability of HCT116 cells could be promoted by PTPN18 overexpression.

PTPN18 knockout cells showed obvious growth inhibition

After we found that PTPN18 overexpression can boost the proliferation of HCT116 cells, it was also necessary to test whether suppressing PTPN18 expression yielded the opposite effects in HCT116 cells. First, we knocked out PTPN18 in HCT116 cells using the CRISPR-Cas9 method, and a Western blot assay was conducted to measure PTPN18 expression (Fig. 3A). Next, we performed a CCK8 assay to test cell growth. The results showed that cell growth was apparently suppressed in PTPN18 knockout cells compared to parental HCT116 cells (Fig. 3B). Next, colony formation and soft agar assays were also performed to examine the proliferation ability, and the clones of HCT116 PTPN18$^{-/-}$ cells were much smaller and fewer than those in control cells (Fig. 3C and E). There were also significantly fewer

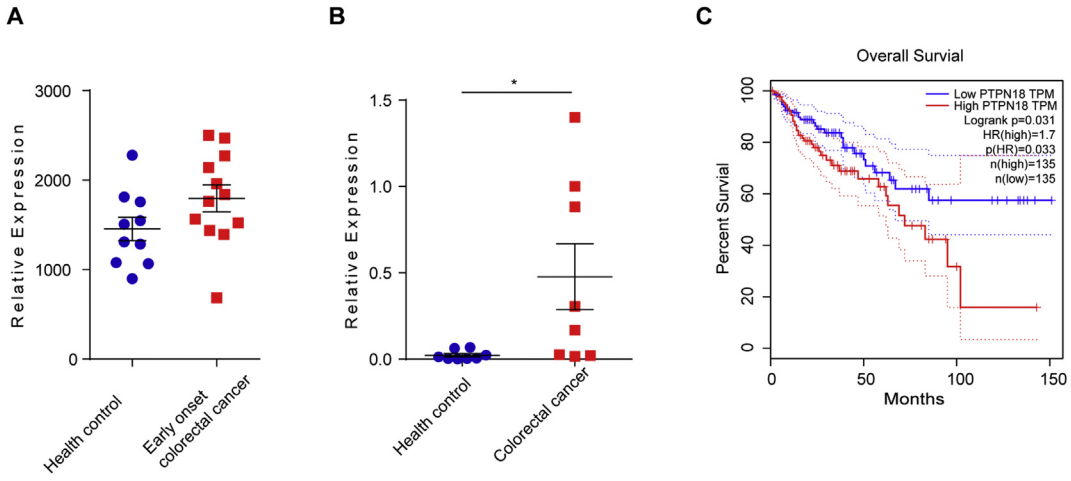

Figure 1 High PTPN18 expression is associated with severe CRC and a low survival rate. **(A)** The data from the GEO database (GSE4107) was searched to compare PTPN18 mRNA expression in early onset CRC and healthy tissues. **(B)** mRNA levels of PTPN18 were measured in CRC and paired normal tissues from 8 patients by real-time PCR. **(C)** A Kaplan–Meier analysis was used to assess the effect of PTPN18 on CRC patient survival. The numbers of CRC patients with high and low PTPN18 expression were both 135. The data were collected from GEPIA (http://gepia.cancer-pku.cn/detail.php?gene=PTPN18). (*, $P < 0.05$).

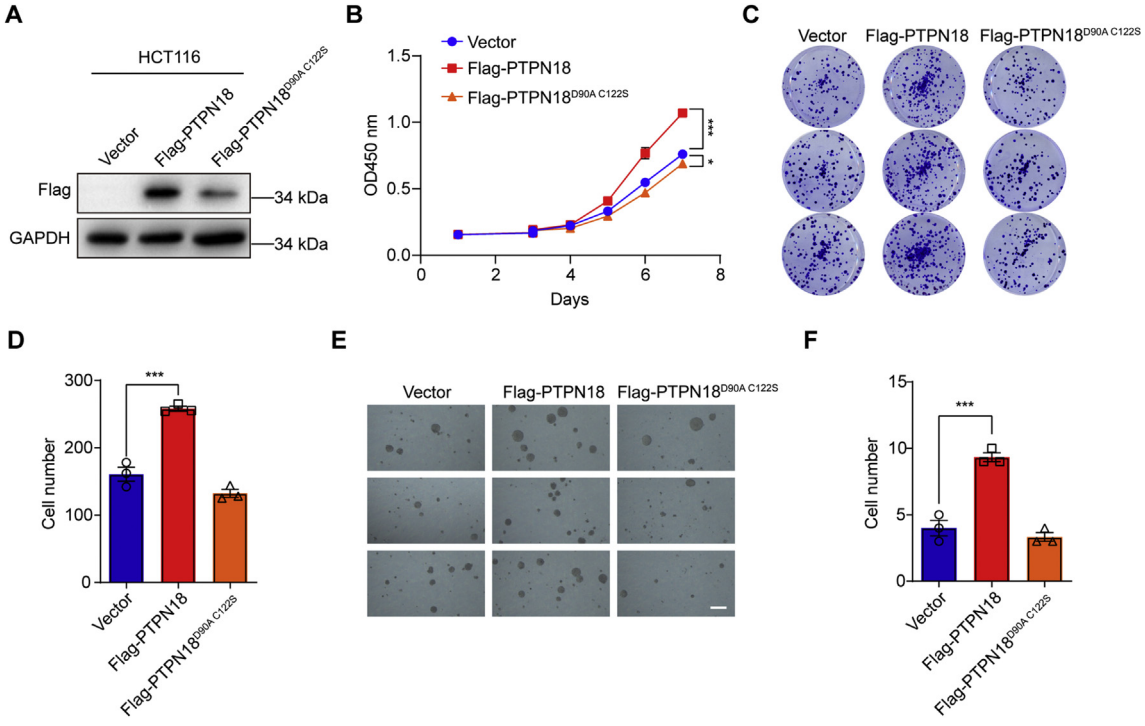

Figure 2 PTPN18 upregulation enhances the proliferation and malignancy of CRC *in vitro*. **(A)** The expression of Flag-PTPN18 and Flag-PTPN18$^{D90A\ C122S}$ was assessed by Western blotting. Lentiviruses were used to construct HCT116 cell lines stably transfected with Flag-PTPN18 and Flag-PTPN18$^{D90A\ C122S}$. **(B)** CCK8 assay was performed to examine the growth and proliferation ability of the Flag-PTPN18-overexpressing, Flag-PTPN18$^{D90A\ C122S}$-overexpressing and control cell lines. **(C)** The proliferation ability of the Flag-PTPN18-overexpressing, Flag-PTPN18$^{D90A\ C122S}$-overexpressing and control cell lines was tested through colony formation assays. **(D)** The cell numbers for the Flag-PTPN18-overexpressing, Flag-PTPN18$^{D90A\ C122S}$-overexpressing and control cell lines in the colony formation assay were counted using ImageJ. **(E)** Soft agar assays were conducted to examine the anchorage-independent growth ability of the Flag-PTPN18-overexpressing, Flag-PTPN18-overexpressing and control cell lines (Scale bar: 200 μm). **(F)** The statistical analysis of the Flag-PTPN18-overexpressing, Flag-PTPN18$^{D90A\ C122S}$-overexpressing and control cell lines for the soft agar assay. (*, $P < 0.05$; ***, $P < 0.001$).

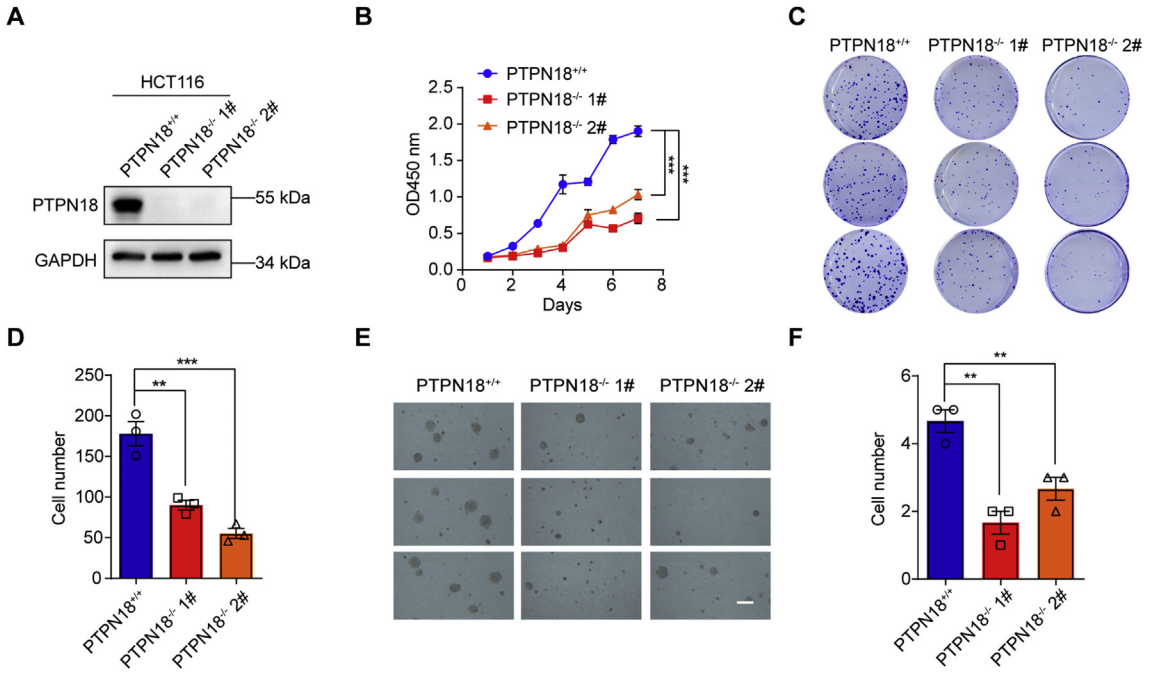

Figure 3 Knocking out PTPN18 inhibits the proliferation of HCT116 cells. **(A)** HCT116 PTPN18$^{-/-}$ cell lines were constructed, and protein expression was detected by Western blotting. **(B)** CCK8 assays were performed to assess the growth and proliferation ability of the HCT116 PTPN18$^{-/-}$ and control cell lines. **(C)** Colony formation assays were conducted to examine the proliferation capacity of the HCT116 PTPN18$^{-/-}$ and control cell lines. **(D)** Cell numbers of the HCT116 PTPN18$^{-/-}$ and control cell lines in the colony formation assays were counted using ImageJ. **(E)** Soft agar assays were performed to assess the anchorage-independent growth ability of the HCT116 PTPN18$^{-/-}$ and control cell lines (Scale bar: 200 μm). **(F)** The statistical analysis of the HCT116 PTPN18$^{-/-}$ and control cell lines for the soft agar assay. (**, $P < 0.01$; ***, $P < 0.001$).

cell numbers for the two HCT116 PTPN18$^{-/-}$ cell lines than the control cell lines (Fig. 3D and F). These data suggest that PTPN18 loss inhibits HCT116 cell proliferation.

PTPN18 promotes MYC signaling pathway activation in CRC

As the phenotype of CRC cells can be obviously influenced by changes in PTPN18 expression, we next explored the mechanism of PTPN18 in CRC. To analyze the variations in gene expression and pathways that PTPN18 could influence, RNA-seq was performed first. We observed the great effect exerted by PTPN18, with hundreds of genes changing in terms of their mRNA levels (Fig. 4A). A principal component analysis also demonstrated this finding (Fig. 4B). The distinctly separate groups indicated that there were significant differences between the HCT116 PTPN18$^{-/-}$ cell line and the control cell line. Specifically, the PI3K-AKT and MAPK signaling pathway exhibited the most significant changes in expression in the absence of PTPN18 (Fig. 4C). After gene set enrichment analysis (GSEA) of the RNA-seq data, we observed that knocking out PTPN18 had a negative effect on several signaling pathways that control cell proliferation and metabolism, including the MYC signaling pathway (Fig. 4D). Moreover, MYC is an important part of PI3k-AKT and MAPK signaling pathway, especially in CRC,[26,27] indicating that the role of PTPN18 in the MYC signaling should be further elucidated.

First, a luciferase assay was conducted to confirm the previous result, and an activating effect was detected when we overexpressed PTPN18 in 293T cells compared to that observed in the control and Flag-PTPN18$^{D90A\ C122S}$-overexpressing cell lines (Fig. 4E). We also assessed MYC luciferase activity to test the effect of PTPN18 knockout in HCT116 cells, and obvious luciferase activity inhibition was observed in the HCT116 PTPN18$^{-/-}$ cell lines (Fig. 4F). In addition, to determine changes in MYC signaling pathways, we examined the expression level of the genes downstream of MYC using real-time PCR. As CDK4 is the most notable downstream gene of MYC and plays a significant role in the cell cycle,[28] we assessed CDK4 mRNA expression in the Flag-PTPN18-overexpressing cell line, the PTPN18$^{-/-}$ cell lines and the corresponding control cell lines. Enhanced expression of CDK4 was found in the PTPN18 overexpressing cell line (Fig. 4G). In contrast, an obvious decrease in CDK4 expression was detected in the PTPN18 knockout cell lines (Fig. 4H). Overall, we deduced that PTPN18 has the capacity to activate the MYC signaling pathway.

PTPN18 interacts with MYC and increases the MYC protein level

After we demonstrated that PTPN18 has a significant impact downstream of the MYC pathway, we explored whether PTPN18 controls the MYC pathway through transcriptional regulation or posttranscriptional regulation. Specifically, we examined the mRNA level of MYC in the

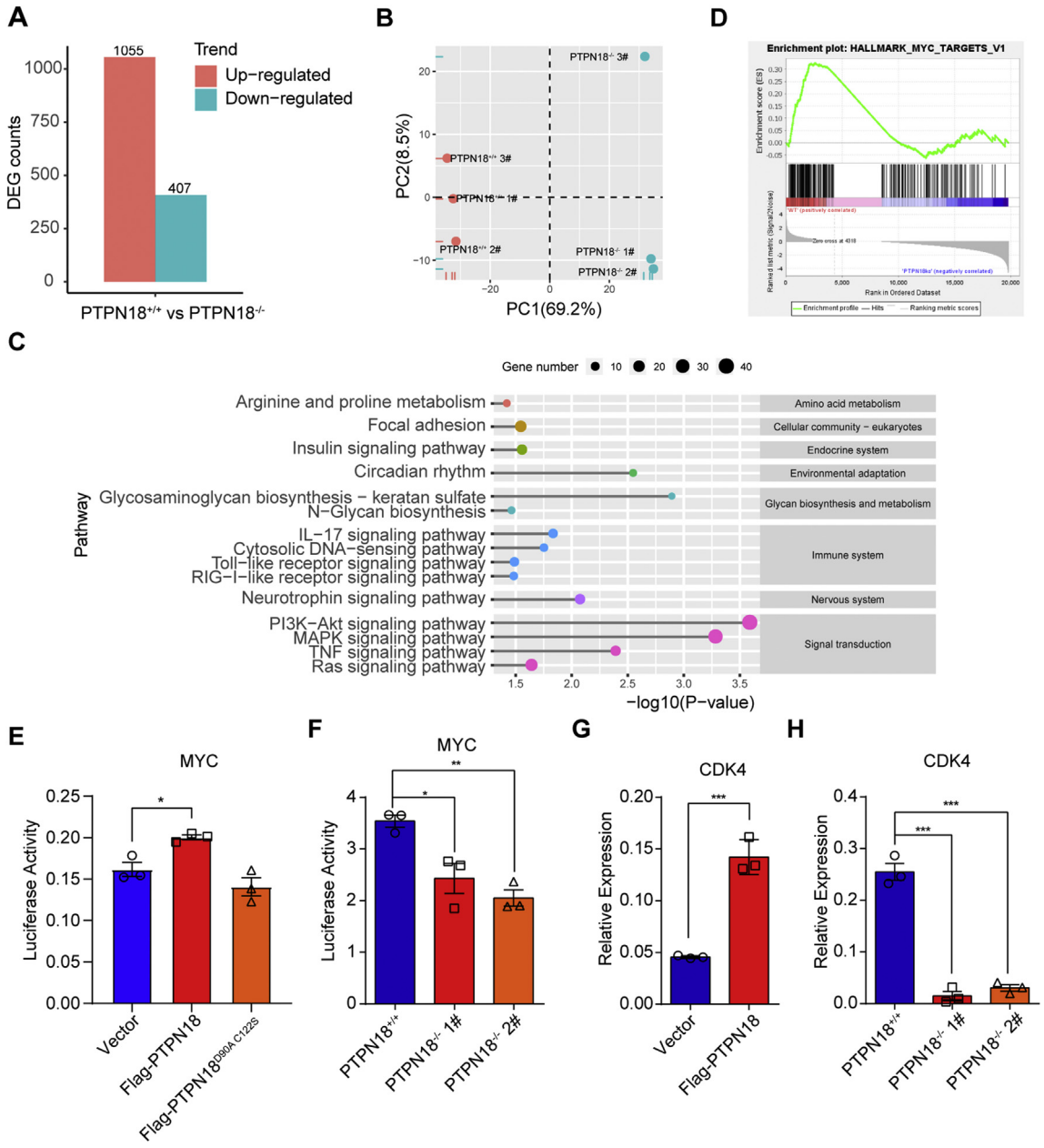

Figure 4 PTPN18 promotes MYC pathway activation. **(A)** RNA-seq was used to examine the changes in gene expression in HCT116 PTPN18$^{-/-}$ cells compared to that observed in the control cells. **(B)** Principal component analysis was performed to test the repeatability in groups of HCT116 PTPN18$^{-/-}$ cells and its control cells and the diversity between the two groups. **(C)** Kyoto Encyclopedia of Genes and Genomes (KEGG) pathway enrichment analysis was conducted to identify the signaling pathways that changed most significantly in the absence of PTPN18. **(D)** GSEA was performed to assess the mRNA changes of genes in the MYC pathway between the HCT116 PTPN18$^{-/-}$ and control groups. **(E)** Luciferase assays were carried out to assess the effect of Flag-PTPN18 and Flag-PTPN18$^{D90A\ C122S}$ overexpression on the MYC pathway in 293T cells. **(F)** Luciferase assays were conducted to examine the effect of PTPN18 loss on the MYC pathway in HCT116 cells. **(G)** Real-time PCR was performed to assess the variation of CDK4 mRNA expression in the Flag-PTPN18-overexpressing in 293T cell line. **(H)** The effect of PTPN18 knockout on CDK4 mRNA levels in HCT116 cells was detected using real-time PCR. (*, $P < 0.05$; **, $P < 0.01$; ***, $P < 0.001$).

Flag-PTPN18-overexpressing cell line and its control cell line, observing that PTPN18 overexpression had almost no effect on MYC mRNA levels (Fig. 5A). Thus, we speculated that PTPN18 regulates the MYC signaling pathway through posttranscriptional regulation in HCT116 cells. First, to determine whether PTPN18 and MYC interact or if MYC is a substrate of PTPN18, we constructed two "substrate-trapping" mutants: PTPN18^{C122S} and PTPN18$^{D90A\ C122S}$. Then, coimmunoprecipitation was performed to assess the interaction between PTPN18 and MYC, and the results revealed that the double mutant (PTPN18$^{D90A\ C122S}$) could interact with MYC (Fig. 5B). Subsequently, we performed an

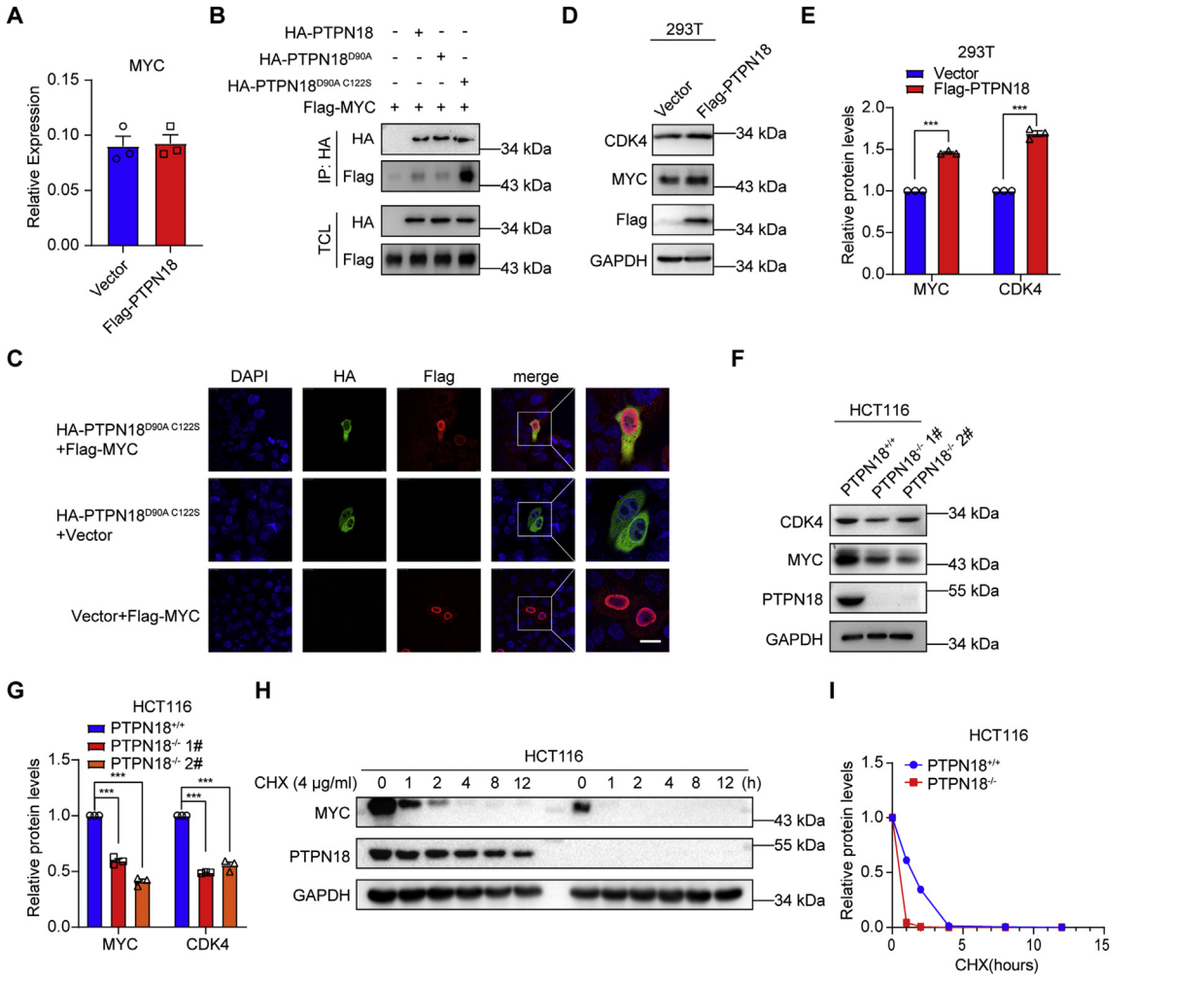

Figure 5 MYC interacts with PTPN18, and PTPN18 affects MYC protein levels. **(A)** Real-time PCR was performed to assess the changes in MYC mRNA expression induced by Flag-PTPN18 overexpression in HCT116 cells. **(B)** "Substrate-trapping" mutants were constructed, and Co-IP was performed to examine the interaction between Flag-MYC and HA-PTPN18, including mutants in 293T cells. **(C)** Colocalization was detected between HA-PTPN18$^{D90A/C122S}$ and Flag-MYC in the cytoplasm of HeLa cells through immunofluorescence assays. The Pearson's coefficient of colocalization (r) was 0.56 (Scale bar: 10 μm). **(D)** The changes in CDK4 and MYC protein levels induced by Flag-PTPN18 overexpression were examined in 293T cells by Western blotting. **(E)** The alterations in CDK4 and MYC protein levels in 293T cells with Flag-PTPN18 overexpression were quantified. **(F)** The changes in CDK4 and MYC protein levels were assessed in HCT116 PTPN18$^{-/-}$ and control cell lines by Western blotting. **(G)** The variation in CDK4 and MYC protein levels in HCT116 PTPN18$^{-/-}$ and control cell lines was quantified. **(H)** The half-life of MYC in HCT116 PTPN18$^{-/-}$ and control cell lines was assessed by CHX assay. **(I)** The relative protein levels of MYC in the CHX assay were qualified. (***, $P < 0.001$).

immunofluorescence assay in HeLa cells and observed colocalization in the cytoplasm of the cells transfected with HA-PTPN18$^{D90A\ C122S}$ and Flag-MYC, whereas no colocalization was detected in the control groups (Fig. 5C). Therefore, we inferred that MYC interacted with PTPN18.

Moreover, the protein level of MYC was influenced by PTPN18. Therefore, we overexpressed PTPN18 in 293T cells and observed that MYC protein levels were higher than those detected in 293T cells transfected with the vector (Fig. 5D and E). We also observed that MYC protein levels were decreased in the HCT116 PTPN18$^{-/-}$ cell lines (Fig. 5F and G). CDK4 was also detected, and our finding was consistent with the previous results. To further assess the influence of PTPN18 on MYC stability, we used a cycloheximide-chase (CHX) assay based on the time course of MYC degradation. The results showed that the half-life of MYC decreased significantly in the absence of PTPN18 in HCT116 cells. Taken together, these data suggest that PTPN18 regulates the MYC pathway by interacting with and stabilizing the MYC protein.

PTPN18 deletion inhibited tumorigenesis in HCT116 cells *in vivo*

To validate the effect of PTPN18 on the tumorigenicity of CRC cells *in vivo*, HCT116 WT cells and HCT116 PTPN18$^{-/-}$ cells were injected subcutaneously into the flanks of nude mice. The mice were sacrificed 4 weeks after injection, and the sizes of the subcutaneous tumors in the HCT116

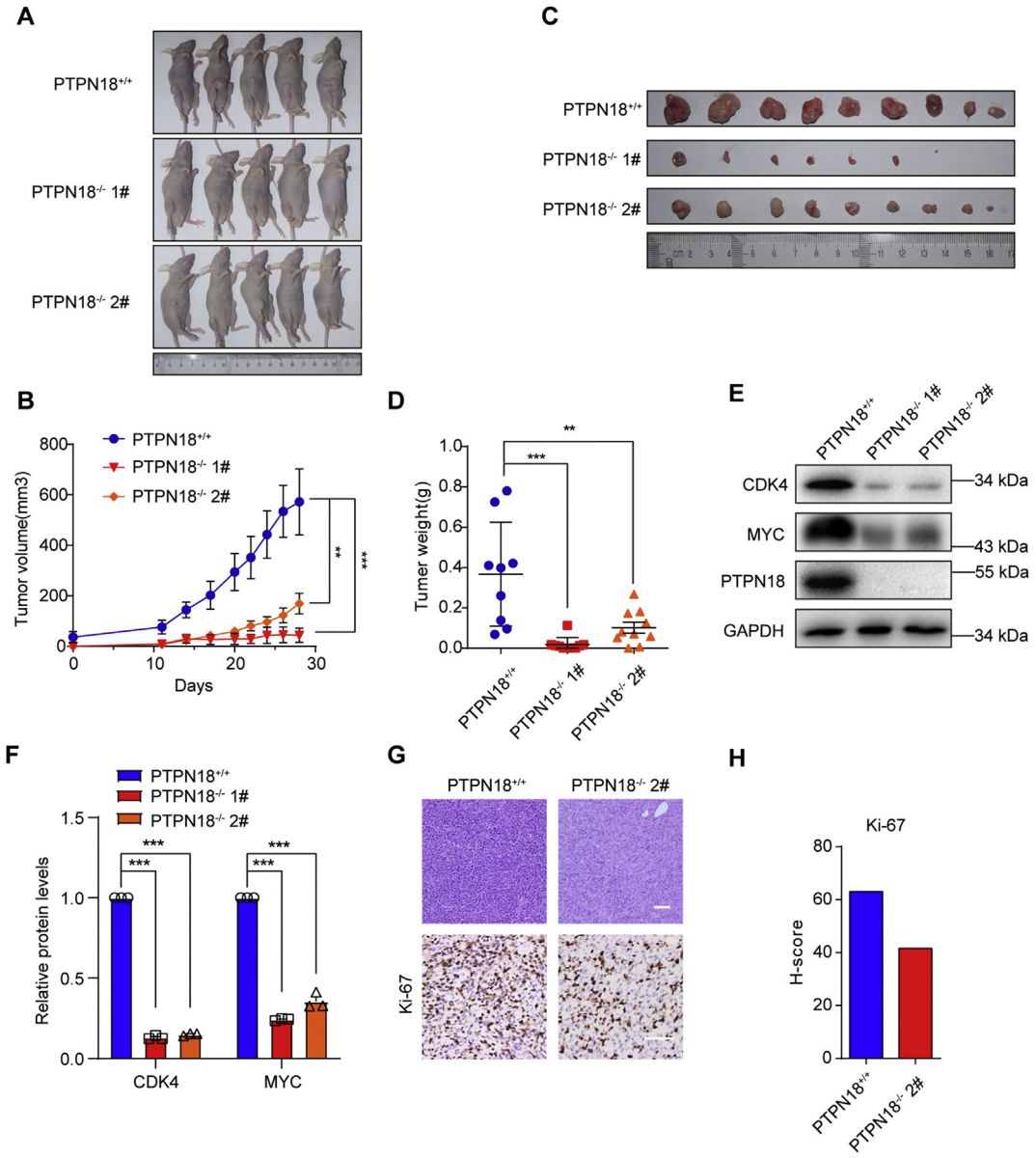

Figure 6 PTPN18 loss represses the tumorigenicity of HCT116 cells. **(A)** The sizes of subcutaneous tumors from nude mice were observed and compared. **(B)** The tumor sizes in the HCT116 PTPN18$^{-/-}$ and control groups were measured using a vernier caliper and recorded regularly. **(C)** and **(D)** Tumor tissues from the HCT116 PTPN18$^{-/-}$ and control groups were collected and weighed. **(E)** PTPN18, MYC and CDK4 protein levels in tumor tissues were assessed by Western blotting. **(F)** The alterations in CDK4 and MYC protein levels in tumor tissues from the HCT116 PTPN18$^{-/-}$ and control groups were quantified. **(G)** Histological analysis of tumor tissues was performed using HE staining (Scale bars: 100 μm). Ki-67 staining was examined in tumor tissues using IHC (Scale bars: 100 μm). **(H)** H-score in IHC assay was calculated. Ki-67 staining was scored as high (3+), moderate (2+), low (1+) and negative (0). The percentage of cells within each tissue core stained at each intensity were recorded to calculate an H-score for each sample. The H-score for staining each sample was defined as: H-score = 0* (% at 0) + 1* (% at 1+) + 2* (% at 2+) + 3* (% at 3+). (**, $P < 0.01$; ***, $P < 0.001$).

PTPN18$^{-/-}$ groups were smaller than those in the HCT116 WT group (Fig. 6A). The average tumor volumes in the HCT116 PTPN18$^{-/-}$ groups were smaller than those in the HCT116 WT group (Fig. 6B). After the tumors were collected and weighed (Fig. 6C), we found that the average xenograft weights in the HCT116 PTPN18$^{-/-}$ groups were sharply reduced (Fig. 6D).

In addition, we extracted protein from the tumors, and CDK4, MYC and PTPN18 expression was assessed by Western blot analysis. We found that the CDK4 and MYC expression decreased significantly in the absence of PTPN18, which was consistent with the previous *in vitro* results (Fig. 6E and F). Furthermore, HE staining and IHC were conducted, and Ki67 expression was shown to be lower in the HCT116 PTPN18$^{-/-}$ group than that observed in the in the HCT116 WT group (Fig. 6G and H). These results demonstrated that inhibiting the expression of PTPN18 has a repressive impact on the tumorigenesis of CRC cells *in vivo*.

Discussion

Previous studies have demonstrated that PTPN18 is a tumor suppressor in breast cancer[29] and hepatocellular carcinoma,[30] while PTPN18 overexpression can promote the development of endometrial cancer.[23] In addition, different PTPs exert different functions in CRC. Specifically, PTPN4,[31] PTPN9,[32] and PTPRT[33] act as tumor suppressors in CRC, while PTPN2[34] can promote tumor development. Nevertheless, very limited studies have been done about the role of PTPN18 in CRC. In the present study, we demonstrated that PTPN18 is overexpressed in CRC. Furthermore, PTPN18 could activate the MYC pathway and increase the protein level of MYC, causing an increase in CDK4 expression and the development of CRC.

Our findings are consistent with those of Ganapati, who demonstrated that PTP-S2 could increase the protein level of MYC without altering its mRNA level and promote cell proliferation,[35] although the mechanism associated with this phenomenon was not described. It is generally acknowledged that the stability of the MYC protein is tightly associated with Thr58 and Ser62.[36–38] Ser62 phosphorylation is required for MYC stabilization, while Thr58 phosphorylation, which depends on prior Ser62 phosphorylation, is associated with MYC degradation.[39] However, few studies have investigated the tyrosine phosphorylation of MYC.

In our present study, we demonstrated that PTPN18 interacts with MYC using a substrate-trapping assay and immunofluorescence. We speculated that MYC is a potential substrate of PTPN18, but we did not find the phosphorylation site of MYC. In addition, the relationship between the tyrosine phosphorylation site of MYC and its stability has not been clarified.

A possible explanation for the result in this article might be that a tyrosine site of MYC could be dephosphorylated by PTPN18, which perhaps has an effect on the phosphorylation of Thr58 and Ser62. In this way, the tyrosine dephosphorylation of MYC would promote the phosphorylation of Ser so that MYC could be stabilized and the downstream target of MYC, CDK4, could be activated.

However, the stability of MYC also depends on its ubiquitination, SUMOylation and acetylation status.[40–42] Therefore, another potential mechanism of the relationship between PTPN18 and MYC is that PTPN18 may dephosphorylate a ubiquitinase, desumoylase or acetylase targeting MYC, which could form a protein complex with PTPN18 and MYC. The dephosphorylation of this ubiquitinase, desumoylase or acetylase would control its activity and regulate MYC by influencing its stability. Our findings may be somewhat limited because the MYC tyrosine dephosphorylation site or other proteins in the PTPN18-MYC complex were not identified, and additional experiments are needed to elucidate this mechanism.

In conclusion, our research demonstrated that PTPN18 could promote tumorigenesis through the MYC pathway and that PTPN18 loss has a significant inhibitory effect on CRC proliferation and malignancy. Our findings suggest that the targeting of PTPN18 is a powerful approach for reducing CRC burden; therefore, considering the limited treatments of CRC at present,[43] PTPN18 could be a new target for the treatment of CRC.

Authors contribution

RL D, XM S, SZ L and C L were responsible for the overall experimental design and analysis. C L completed the experiments in Fig. 1–6 in collaboration with other authors. All authors contributed to writing or editing of the manuscript.

Conflict of Interests

Authors declare no conflict of interests.

Acknowledgements

This work was supported by grants from the National Natural Science Foundation of China (NSFC) [grant numbers 81872271 and 81902844], Translational Medicine and Interdisciplinary Research Joint Fund of Zhongnan Hospital of Wuhan University [grant number ZNJC201921] and Zhongnan Hospital of Wuhan University Science, Technology and Innovation Seed Fund [grant number znpy2018102].

References

1. Brody H. Colorectal cancer. *Nature*. 2015;521(7551),S1.
2. Marmol I, Sanchez-de-Diego C, Pradilla Dieste A, Cerrada E, Rodriguez Yoldi MJ. Colorectal carcinoma: a general overview and future perspectives in colorectal cancer. *Int J Mol Sci*. 2017;18(1),e197.
3. Cunningham D, Atkin W, Lenz HJ, et al. Colorectal cancer. *Lancet*. 2010;375(9719):1030–1047.
4. Cancer Genome Atlas Network. Comprehensive molecular characterization of human colon and rectal cancer. *Nature*. 2012;487(7407):330–337.
5. Wood LD, Parsons DW, Jones S, et al. The genomic landscapes of human breast and colorectal cancers. *Science*. 2007;318(5853):1108–1113.
6. Brocardo M, Henderson BR. APC shuttling to the membrane, nucleus and beyond. *Trends Cell Biol*. 2008;18(12):587–596.
7. Mohammed MK, Shao C, Wang J, et al. Wnt/beta-catenin signaling plays an ever-expanding role in stem cell self-renewal, tumorigenesis and cancer chemoresistance. *Genes Dis*. 2016;3(1):11–40.
8. Herzig DO, Tsikitis VL. Molecular markers for colon diagnosis, prognosis and targeted therapy. *J Surg Oncol*. 2015;111(1):96–102.
9. Rennoll S, Yochum G. Regulation of MYC gene expression by aberrant Wnt/beta-catenin signaling in colorectal cancer. *World J Biol Chem*. 2015;6(4):290–300.
10. Myant K, Sansom O. Efficient Wnt mediated intestinal hyperproliferation requires the cyclin D2-CDK4/6 complex. *Cell Div*. 2011;6(1),e3.
11. Sato K, Masuda T, Hu Q, et al. Novel oncogene 5MP1 reprograms c-Myc translation initiation to drive malignant phenotypes in colorectal cancer. *EBioMedicine*. 2019;44:387–402.
12. Wang L, Xue M, Chung DC. c-Myc is regulated by HIF-2alpha in chronic hypoxia and influences sensitivity to 5-FU in colon cancer. *Oncotarget*. 2016;7(48):78910–78917.
13. Satoh K, Yachida S, Sugimoto M, et al. Global metabolic reprogramming of colorectal cancer occurs at adenoma stage and is induced by MYC. *Proc Natl Acad Sci U S A*. 2017;114(37):E7697–E7706.

14. Sears R, Nuckolls F, Haura E, Taya Y, Tamai K, Nevins JR. Multiple Ras-dependent phosphorylation pathways regulate Myc protein stability. *Genes Dev*. 2000;14(19):2501—2514.
15. Alonso A, Pulido R. The extended human PTPome: a growing tyrosine phosphatase family. *FEBS J*. 2016;283(11):2197—2201.
16. Du Y, Grandis JR. Receptor-type protein tyrosine phosphatases in cancer. *Chin J Cancer*. 2015;34(2):61—69.
17. Laczmanska I, Sasiadek MM. Tyrosine phosphatases as a superfamily of tumor suppressors in colorectal cancer. *Acta Biochim Pol*. 2011;58(4):467—470.
18. Veillette A, Rhee I, Souza CM, Davidson D. PEST family phosphatases in immunity, autoimmunity, and autoinflammatory disorders. *Immunol Rev*. 2009;228(1):312—324.
19. Wang HM, Xu YF, Ning SL, et al. The catalytic region and PEST domain of PTPN18 distinctly regulate the HER2 phosphorylation and ubiquitination barcodes. *Cell Res*. 2014;24(9):1067—1090.
20. Gensler M, Buschbeck M, Ullrich A. Negative regulation of HER2 signaling by the PEST-type protein-tyrosine phosphatase BDP1. *J Biol Chem*. 2004;279(13):12110—12116.
21. Doody KM, Bottini N. "PEST control": regulation of molecular barcodes by tyrosine phosphatases. *Cell Res*. 2014;24(9):1027—1028.
22. Huang WK, Akçakaya P, Gangaev A, et al. miR-125a-5p regulation increases phosphorylation of FAK that contributes to imatinib resistance in gastrointestinal stromal tumors. *Exp Cell Res*. 2018;371(1):287—296.
23. Cai J, Huang S, Yi Y, Bao S. Downregulation of PTPN18 can inhibit proliferation and metastasis and promote apoptosis of endometrial cancer. *Clin Exp Pharmacol Physiol*. 2019;46(8):734—742.
24. Zhao H, Pan WM, Zhang HH, et al. Cancer testis antigen 55 deficiency attenuates colitis-associated colorectal cancer by inhibiting NF-kappaB signaling. *Cell Death Dis*. 2019;10(4),e304.
25. Blanchetot C, Chagnon M, Dubé N, Hallé M, Tremblay ML. Substrate-trapping techniques in the identification of cellular PTP targets. *Methods*. 2005;35(1):44—53.
26. Muranen T, Selfors LM, Hwang J, et al. ERK and p38 MAPK activities determine sensitivity to PI3K/mTOR inhibition via regulation of MYC and YAP. *Cancer Res*. 2016;76(24):7168—7180.
27. Setia S, Nehru B, Sanyal SN. Upregulation of MAPK/Erk and PI3K/Akt pathways in ulcerative colitis-associated colon cancer. *Biomed Pharmacother*. 2014;68(8):1023—1029.
28. Dang CV. MYC on the path to cancer. *Cell*. 2012;149(1):22—35.
29. Lucci MA, Orlandi R, Triulzi T, Tagliabue E, Balsari A, Villa-Moruzzi E. Expression profile of tyrosine phosphatases in HER2 breast cancer cells and tumors. *Cell Oncol*. 2010;32(5—6):361—372.
30. Zhangyuan G, Yin Y, Zhang W, et al. Prognostic value of phosphotyrosine phosphatases in hepatocellular carcinoma. *Cell Physiol Biochem*. 2018;46(6):2335—2346.
31. Zhang BD, Li YR, Ding LD, Wang YY, Liu HY, Jia BQ. Loss of PTPN4 activates STAT3 to promote the tumor growth in rectal cancer. *Cancer Sci*. 2019;110(7):2258—2272.
32. Wang D, Cheng Z, Zhao M, et al. PTPN9 induces cell apoptosis by mitigating the activation of Stat3 and acts as a tumor suppressor in colorectal cancer. *Cancer Manag Res*. 2019;11:1309—1319.
33. Zhang X, Guo A, Yu J, et al. Identification of STAT3 as a substrate of receptor protein tyrosine phosphatase T. *Proc Natl Acad Sci U S A*. 2007;104(10):4060—4064.
34. Spalinger MR, Manzini R, Hering L, et al. PTPN2 regulates inflammasome activation and controls onset of intestinal inflammation and colon cancer. *Cell Rep*. 2018;22(7):1835—1848.
35. Ganapati U, Gupta S, Radha V, Sudhakar C, Manogaran PS, Swarup G. A nuclear protein tyrosine phosphatase induces shortening of G1 phase and increase in c-Myc protein level. *Exp Cell Res*. 2001;265(1):1—10.
36. An J, Yang DY, Xu QZ, et al. DNA-dependent protein kinase catalytic subunit modulates the stability of c-Myc oncoprotein. *Mol Cancer*. 2008;7,e32.
37. Tsai WB, Aiba I, Long Y, et al. Activation of Ras/PI3K/ERK pathway induces c-Myc stabilization to upregulate argininosuccinate synthetase, leading to arginine deiminase resistance in melanoma cells. *Cancer Res*. 2012;72(10):2622—2633.
38. Jiang G, Huang C, Liao X, et al. The RING domain in the antiapoptotic protein XIAP stabilizes c-Myc protein and preserves anchorage-independent growth of bladder cancer cells. *J Biol Chem*. 2019;294(15):5935—5944.
39. Zhang L, Zhou H, Li X, et al. Eya3 partners with PP2A to induce c-Myc stabilization and tumor progression. *Nat Commun*. 2018;9(1):1047.
40. Vervoorts J, Lüscher-Firzlaff JM, Rottmann S, et al. Stimulation of c-MYC transcriptional activity and acetylation by recruitment of the cofactor CBP. *EMBO Rep*. 2003;4(5):484—490.
41. Farrell AS, Sears RC. MYC degradation. *Cold Spring Harb Perspect Med*. 2014;4(3),a014365.
42. Chen Y, Sun XX, Sears RC, Dai MS. Writing and erasing MYC ubiquitination and SUMOylation. *Genes Dis*. 2019;6(4):359—371.
43. Wang YJ, Fletcher R, Yu J, Zhang L. Immunogenic effects of chemotherapy-induced tumor cell death. *Genes Dis*. 2018;5(3):194—203.